J. of Supercritical Fluids 58 (2011) 272–278

Contents lists available at ScienceDirect

The Journal of Supercritical Fluids

journal homepage: www.elsevier.com/locate/supflu

A study of solvation of o-/m-hydroxybenzoic acid in supercritical CO_2–methanol co-solvent system based on intermolecular interaction by molecular dynamics simulation

Jinyao Wang[a,b,d], Zhijian Wu[c,*], Fengyu Zhao[a,b,**]

[a] State Key Laboratory of Electroanalytical Chemistry, Changchun Institute of Applied Chemistry, Chinese Academy of Sciences, Changchun 130022, PR China
[b] Laboratory of Green Chemistry and Process Changchun Institute of Applied Chemistry, Chinese Academy of Sciences, Changchun 130022, PR China
[c] State Key Laboratory of Rare Earth Resource Utilization, Changchun Institute of Applied Chemistry, Chinese Academy of Sciences, Changchun 130022, PR China
[d] Graduate School, Chinese Academy of Sciences, Beijing 100049, PR China

ARTICLE INFO

Article history:
Received 5 January 2011
Received in revised form 20 June 2011
Accepted 20 June 2011

Keywords:
Supercritical carbon dioxide
Solubility
Hydrogen bonding
Molecular dynamics simulation

ABSTRACT

Solvation behavior of o-hydroxybenzoic acid (o-HBA) and m-hydroxybenzoic acid (m-HBA) in CO_2 and methanol mixtures was investigated by molecular dynamics simulation. The results indicated that the distribution of methanol around o-, m-HBA molecules was different, and it was ascribed to the different hydrogen bonding numbers formed between methanol and HBA molecules. Moreover, the interaction or hydrogen bonds between m-HBA and methanol was much stronger than that between o-HBA and methanol, and with the increasing of CO_2 pressure, it did not change for the former, but decreased for the latter. In addition, the local mole fraction enhancement was also studied. It was demonstrated that the methanol molecules become less aggregate with increasing CO_2 pressure.

1. Introduction

Supercritical fluids (SCF) are very useful solvents in the extraction and fractionation of organic substances because the fluid density can be tuned over a wide range by slightly changing the pressure and temperature [1–4]. However, the relatively high pressure and low solvent ability discourage their applications. It is well-known that the addition of a co-solvent to a SCF often leads to an enhancement of the solubility of a solute [5,6]. A general explanation is that the specific interactions between co-solvent and solute alter the solubility of SCF, based on the results of spectroscopic studies [7–9] and molecular simulation [10,11]. For example, Yamamoto et al. measured Fourier transform infrared (FTIR) spectra of carboxylic acid in supercritical CO_2 ($scCO_2$) and confirmed that the solubility enhancement by ethanol as an entrainer in $scCO_2$ relates to the amount of hydrogen bonding between carboxylic and ethanol [7]. In addition, the structure and interaction between co-solvents and solutes in supercritical fluids were studied with fluorescence and UV absorption experiments by Tomasko et al. [8], and the results suggested that the co-solvent could be used to tailor supercritical fluid solvents by increasing solvent polarity and forming the specific interaction with solutes. Anderson and Siepmann used Monte Carlo simulations to investigate the effect of pressure and the addition of entrainers like n-octane and methanol on the solubility of low-volatility species in CO_2 [10]. They reported that the presence of an entrainer could enhance the solubility of solute, in particular for the solute which has a similar polarity to the entrainer. Till now, although the solubility enhancement in $scCO_2$ by co-solvent has been studied extensively, the effect of solute structure on the enhancement of solubility was less explored. Gohres et al. have used absorption spectra and molecular dynamics (MD) simulation to investigate the solvation of five heterocyclic molecules in CO_2-expanded methanol and demonstrated the importance of solute structure for solvation [12].

In this study, o-HBA and m-HBA, which are shown in Fig. 1, were chosen as model solutes by virtue of the available solubility data in CO_2–methanol co-solvent system [13]. The solubility of m-HBA in $scCO_2$ at 328 K was enhanced by more than two orders of magnitude with the addition of 3.5 mol% methanol, while the enhancement for o-HBA was only one order of magnitude. Furthermore, the solubilities increase with the increase of CO_2 pressure, but their enhancement decreases, indicating that the functional group and steric position of solutes are very important

* Corresponding author. Tel.: +86 0431 85262410; fax: +86 0431 85262410.
** Corresponding author at: State Key Laboratory of Electroanalytical Chemistry, Changchun Institute of Applied Chemistry, Chinese Academy of Sciences, Changchun 130022, PR China. Tel.: +86 0431 85262410; fax: +86 0431 85262410.
E-mail addresses: zjwu@ciac.jl.cn (Z. Wu), zhaofy@ciac.jl.cn (F. Zhao).

0896-8446/$ – see front matter © 2011 Elsevier B.V. All rights reserved.
doi:10.1016/j.supflu.2011.06.008

in governing their solubility. It was assumed that the difference in the solubility enhancement might be ascribed to the difference of the intra/intermolecular hydrogen bondings among HBA and/or methanol molecules. Therefore, the main objective of this work is to shed light on the interaction and solvation structure of co-solvent around solutes with different steric structures by MD simulation. Our results provide a clear explanation for the difference of enhancement of solubility of m-/o-HBA in $scCO_2$ with the addition of methanol.

2. Computation details

Molecular dynamics (MD) simulations were performed using the Gromacs 4.0.4 software package [14–18]. The studied system is based on an equilibrated cubic, periodic simulation box containing 1 solute molecule, 350 methanol and 9650 CO_2 molecules. For CO_2 solvent, the "EMP2" potential parameters were used, which were constructed to reproduce the coexistence curve of the real CO_2 fluids [19]. The united-atom version of the transferable potential for phase equilibra (TraPPE-UA) force field was used to model the methanol molecule [20]. In the TraPPE-UA, the methyl groups were represented by pseudo-atoms placing at the carbon sites, and the oxygen and hydrogen in hydroxyl were modeled explicitly. For the o-HBA and m-HBA molecules, the OPLS-AA force field was used [21]. The intramolecular interactions were modeled using constraints for the bonds, while the harmonic potentials for angular degrees of freedom can be expressed as:

$$U_{\text{angle}}(\theta) = \frac{1}{2}k(\theta - \theta_0)^2 \quad (1)$$

where k, θ, and θ_0 are the force constant, bending angle, and equilibrium bending angle. The dihedral angle potentials for torsional interaction is:

$$U_{\text{dihebral}}(\theta) = \frac{1}{2}a_1(1+\cos(\phi)) + \frac{1}{2}a_2(1-\cos(2\phi)) + \frac{1}{2}a_3(1+\cos(3\phi)) \quad (2)$$

where a_i and ϕ are the force constant and equilibrium torsion angle, respectively. Periodic boundary conditions (PBCs) were used throughout, coulombic interactions were handled using the Ewald summation method.

The simulations were performed on 10 ns in the NPT ensemble at constant temperature 328 K and pressures 10, 14, 20 MPa for o-HBA and 14, 20, 30 MPa for m-HBA in order to obtain the average box length. The value of the box length was used to carry out further MD simulations under constant NVT conditions using a Nose-Hoover thermostat. The equations of motion were integrated using a leapfrog scheme with a 1 fs time step. This simulation data were obtained in production run of 3 ns that were started after an equilibration period of 1 ns. To estimate statistical errors, each MD production run was divided into three consecutive blocks. Values calculated from these blocks were used to estimate standard deviation.

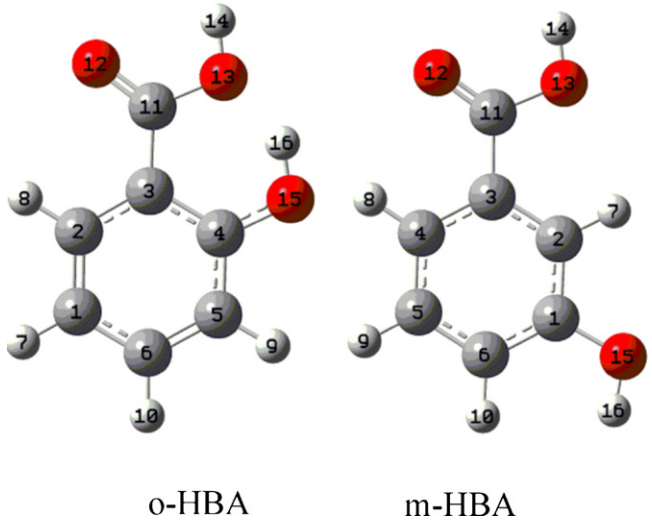

Fig. 1. Structure of the solutes with all the atoms numbered.

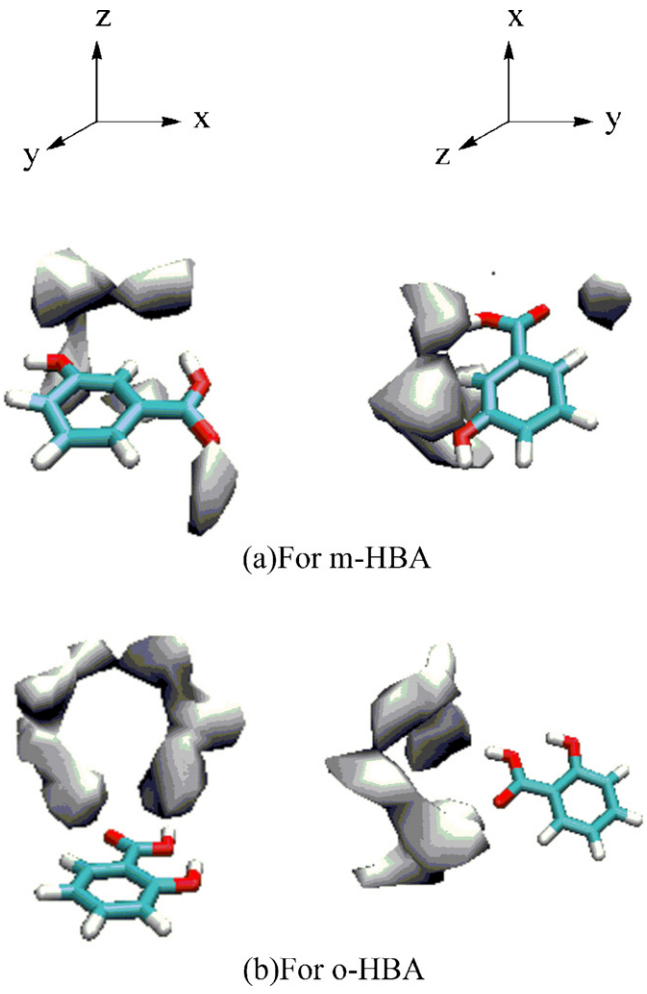

Fig. 2. SDFs of methanol around m-HBA (a) and o-HBA (b) at 14 MPa and 328 K. The SDFs are drawn at an isosurface value of 330.

3. Results and discussion

3.1. Preferential solvation

One mechanism proposed for the solubility enhancement in CO_2–methanol system is that the co-solvent, methanol, may form favorable clusters around solute in CO_2 [22]. In literature, the MD simulation was usually used to provide the local solvation structures via spatial distribution functions (SDFs), which gives the direct information of an atom in the three-dimensional space around a center molecule [23,24]. Fig. 2 is the SDFs of methanol around o-HBA and m-HBA in the presence of 14 MPa CO_2 at 328 K. It clearly shows that for m-HBA, the methanol molecules aggregated around both the carboxyl and hydroxyl groups of m-HBA (Fig. 2a). A quite different distribution was found for o-HBA (Fig. 2b), in which the methanol molecules mainly distributed in the vicinity of carboxyl group with a ring shape cluster. This is not surpris-

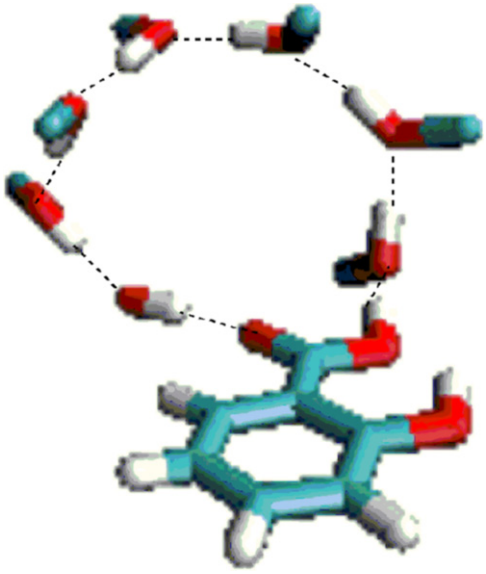

Fig. 3. Snapshot of methanol hydrogen-bonded cluster with o-HBA that was taken from MD simulation at pressure 14 MPa and temperature 328 K (oxygen in red, hydrogen in white and carbon in cyan), and dot lines indicate the presence of hydrogen bonding between neighboring molecules. (For interpretation of the references to color in this figure legend, the reader is referred to the web version of this article.)

ing because a methanol molecule has one hydroxyl group, which can form intermolecular hydrogen-bonded methanol, forming a ring cluster around carboxyl group of o-HBA (Fig. 3). The difference of the methanol distribution around m-HBA and o-HBA should ascribe to their different structures, which will be discussed later.

In order to get further insight into the solvation structures of methanol around HBA isomers, the radial distribution functions (RDFs) for methanol around the carboxyl group and hydroxyl group of m-/o-HBA were calculated at 14 MPa and 328 K (Fig. 4). It is easy to find that the RDFs for methanol around carboxyl group of o-HBA (Fig. 4a) and m-HBA (Fig. 4c) were very similar. The most pronounced peak is H14-OH (for atom labels see Fig. 1) RDF for the oxygen (OH) of methanol around the hydrogen (H14) of carboxyl group located at ~0.16 nm. The second peak is O12-HO RDF for the hydrogen (HO) of hydroxyl group in methanol around the oxygen (O12) of carbonyl group located at ~0.17 nm. Both of the above distances are located in the range of typical hydrogen bond ($rO\cdots H \leq 2.6$ Å) [25]. The peak height for m-HBA (200–270 in Fig. 4c) is a little higher than that for o-HBA (190–270 in Fig. 4a), indicating that more hydrogen bonds were formed between methanol and carboxyl group of m-HBA compared to those with o-HBA.

In contrast, the RDFs for methanol around hydroxyl group of o-HBA (Fig. 4b) and m-HBA (Fig. 4d) are remarkably different. For o-HBA, most of the methanol molecules distributed far from 0.4 nm to the O15 or H16 of hydroxyl group, which was out of hydrogen bond distance. While for the m-HBA, most of the methanol molecules appeared within 0.2 nm around O15 and H16 of hydroxyl group, which means that the typical hydrogen bond was formed between them. Moreover, the peak heights are ~325 and ~225, respectively, higher than those of methanol around the carboxyl group, suggesting that the hydrogen bonds formed between methanol and hydroxyl group was much stronger than those between methanol and the carboxyl group in the m-HBA molecules. By contrast, for o-HBA the hydrogen bonds mainly formed between methanol and the carboxyl groups of o-HBA, but very less with hydroxyl group. These are in agreement with the SDFs shown in Fig. 2, in which the methanol molecules aggregated only around carboxyl group of o-HBA, while they aggregated around both the carboxyl and hydroxyl groups of m-HBA. From the location of the first peak of RDFs for m-HBA and o-HBA, it was demonstrated that the co-solvent methanol distribution in $scCO_2$ was via hydrogen bonding interaction. A more detailed analysis of hydrogen bonding is provided in the following section.

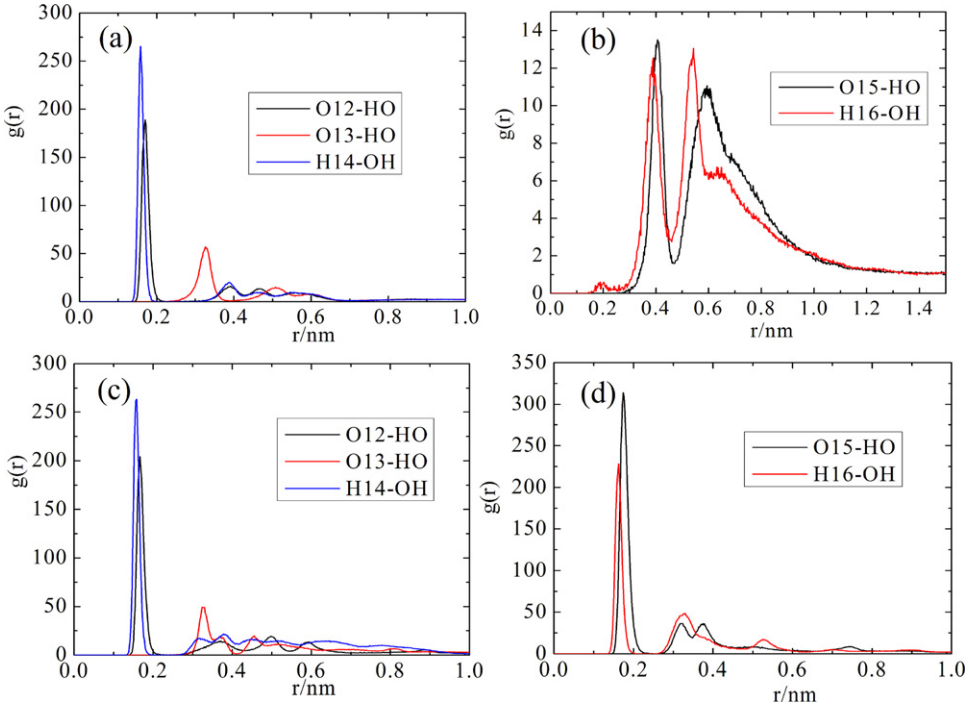

Fig. 4. Radial distribution function (RDF) for methanol surrounding (a) carboxyl group of o-HBA, (b) hydroxyl group of o-HBA, (c) carboxyl group of m-HBA, and (d) hydroxyl group of m-HBA at 14 MPa and 328 K. O12-HO is the hydrogen (HO) of methanol distributed around the oxygen (O12) of carboxyl group; and O13-HO is that around oxygen (O13) of carboxyl group. H14-OH is oxygen of methanol (OH) around hydrogen (H14) of carboxyl. O15-HO is methanol hydrogen (OH) around hydroxyl oxygen (O15) and H16-OH is methanol oxygen (OH) around hydroxyl hydrogen (H16).

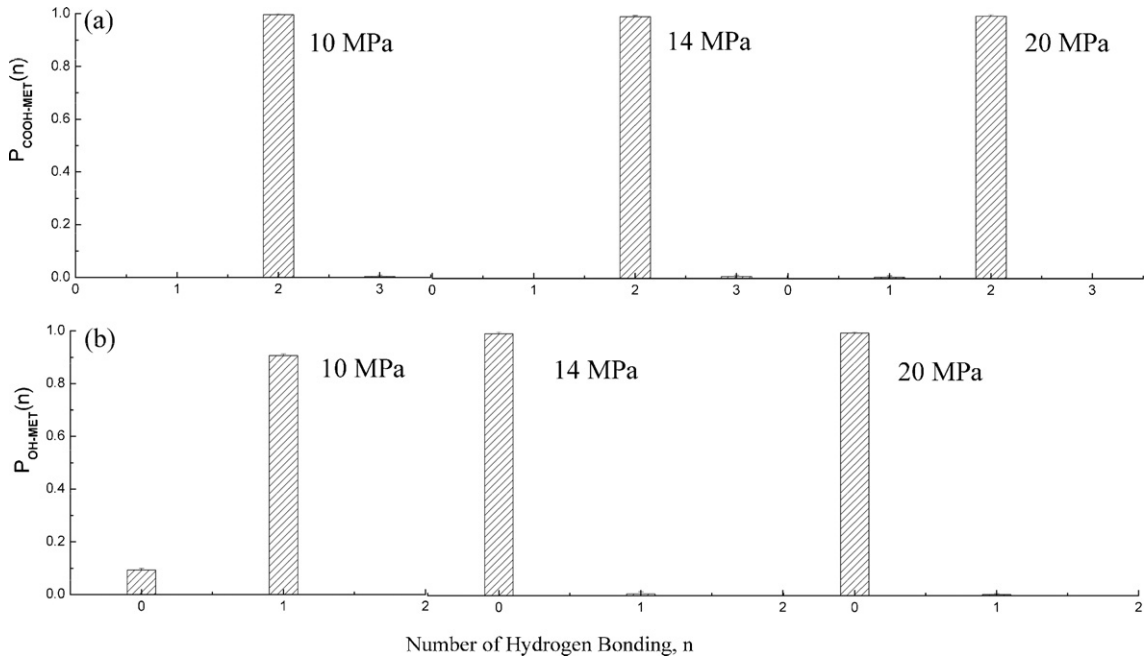

Fig. 5. Distribution of hydrogen bonding number, P(n), between o-HBA and methanol molecules at pressures 10, 14 and 20 MPa. (a) $P_{COOH-MET}(n)$: the hydrogen bonding between carboxyl group (COOH) of o-HBA and methanol (MET). (b) $P_{OH-MET}(n)$: the hydrogen bonding between hydroxyl group (OH) of o-HBA and methanol (MET). The error bar for the data presented was estimated and it was less than 0.6%.

3.2. Hydrogen bonding

By using a definition of hydrogen bonding between two molecules with the following geometric criteria: $rO\cdots O \leq 3.5$ Å, $rO\cdots H \leq 2.6$ Å, and $\angle H–O\cdots O \leq 30°$ [25], the distribution of hydrogen bonding number between o/m-HBA and methanol molecules, P(n), and the number of hydrogen bonding, n, were estimated at different pressures and shown in Figs. 5 and 6, respectively. For o-HBA, it is found that the P(2) was ~99% at all the pressures examined (Fig. 5a). This means that two hydrogen bonds were formed between the carboxyl group of o-HBA and methanol. The same situation was also found for m-HBA (Fig. 6a). On the other hand, in Fig. 5b, it is noted that P(1) had a considerable proportion at 10 MPa, but P(0) became dominant with the pressure increasing from 14 MPa to 20 MPa. This indicates that hydrogen bonding did not exist between hydroxyl group of o-HBA and methanol

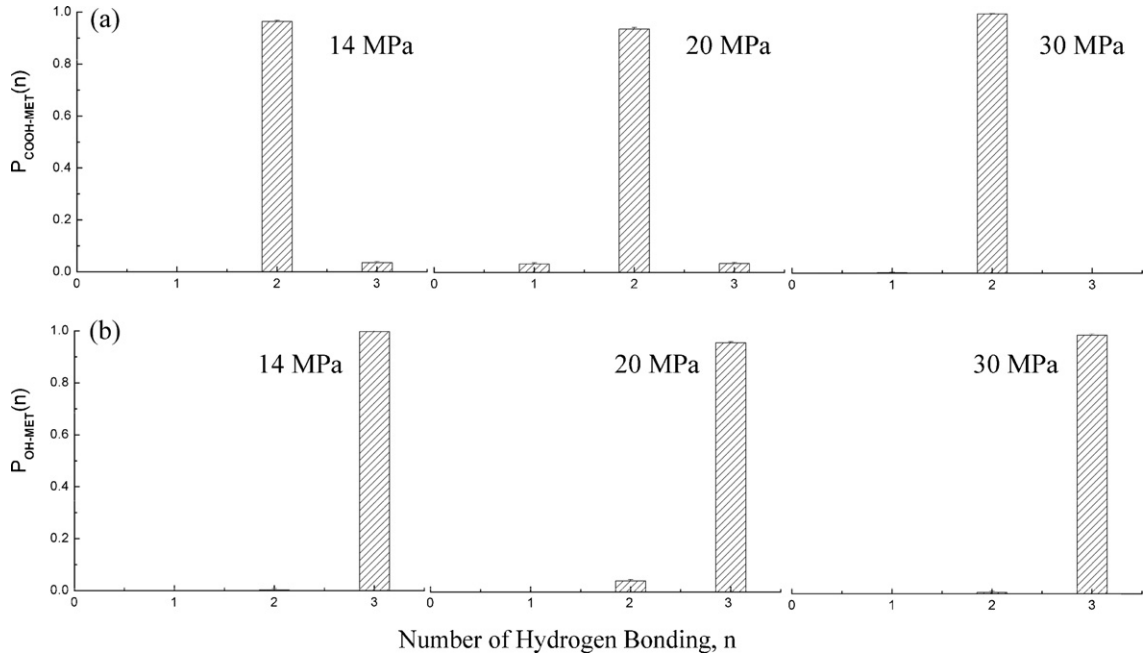

Fig. 6. Distribution of hydrogen bonding number, P(n), between m-HBA and methanol molecules at pressures 14, 20 and 30 MPa. (a) $P_{COOH-MET}(n)$: the hydrogen bonding between carboxyl group (COOH) of m-HBA and methanol (MET). (b) $P_{OH-MET}(n)$: the hydrogen bonding between hydroxyl group (OH) of m-HBA and methanol (MET). The error bar for the data presented was estimated and it was less than 0.6%.

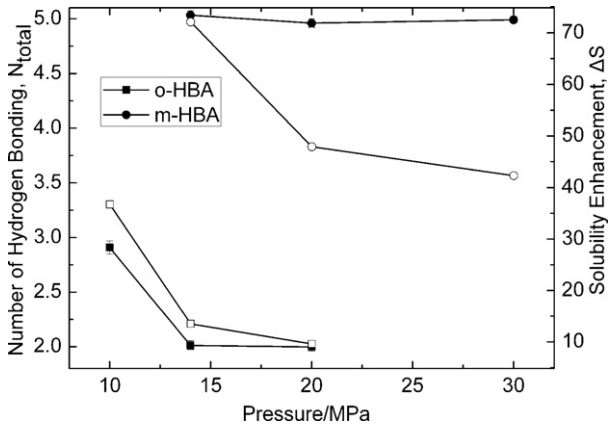

Fig. 7. Total number of hydrogen bonding, N_{total}, between HBA and methanol molecules at different pressures (full symbols). Open symbols: value of solubility enhancement, ΔS, for HBA in CO_2–methanol co-solvent system [13].

molecules at pressures above 14 MPa. In contrast, in Fig. 6b, we found that P(3) reached ~99% and has only a tiny change with the increase of pressure, indicating that there are three hydrogen bonds between hydroxyl group of m-HBA and methanol. The difference of hydrogen bonding numbers for hydroxyl group in o-HBA and m-HBA may be resulted from the intramolecular hydrogen bonding, which exists between hydroxyl and carboxyl in o-HBA molecules, inducing a decrease in the intermolecular hydrogen bonding between hydroxyl group and methanol molecules, while it is opposite for m-HBA.

The total hydrogen bonding number, N_{total}, was calculated from $P_{COOH-MET}(n)$ and $P_{OH-MET}(n)$, as shown in Fig. 7. It was found that the total hydrogen bonding number between m-HBA and methanol was larger than that between o-HBA and methanol, suggesting that the interaction between m-HBA and methanol was stronger than that between o-HBA and methanol. This may be a good explanation for the fact that the enhancement of solubility of m-HBA is higher than that of o-HBA in CO_2–methanol co-solvent system. The difference of total hydrogen bonding numbers is mainly from the hydrogen bonding numbers between hydroxyl group and methanol, which can be seen in Figs. 5b and 6b. Moreover, it is also observed that for m-HBA the value of N_{total} was almost the same with the increase of pressure, but for o-HBA the N_{total} decreases, indicating that the interactions between o-HBA and methanol were weakened by the increase of pressure.

The solubility enhancement values, ΔS (Fig. 7), which are defined as the ratio of the solubility obtained with the presence of cosolvent ethanol to that obtained within neat CO_2 [13]. Comparing ΔS with N_{total}, it can be seen that with the increase in pressure, both N_{total} and ΔS decrease for o-HBA, while for m-HBA, ΔS decreases, but nearly no change for N_{total}. This demonstrated that the decrease of hydrogen bonding number is an important factor for decreasing the enhancement of solubility of o-HBA.

o-HBA has less opportunity to form the dimer due to the intramolecular interaction between carboxyl group and hydroxyl group, but m-HBA prefers to form dimer. Thus, we also simulated the system containing 2 m-HBA molecule, 350 methanol and 9650 CO_2 molecules at 30 MPa and 328 K. The distribution of hydrogen bonding number of m-HBA is calculated and shown in Supporting Information (Fig. S1 and S2). The results show that distribution of hydrogen bonding number of system containing 2 m-HBA is same as that of the system containing 1 m-HBA molecule (Fig. 6). This might suggest that the interaction between solute and solute could be negligible.

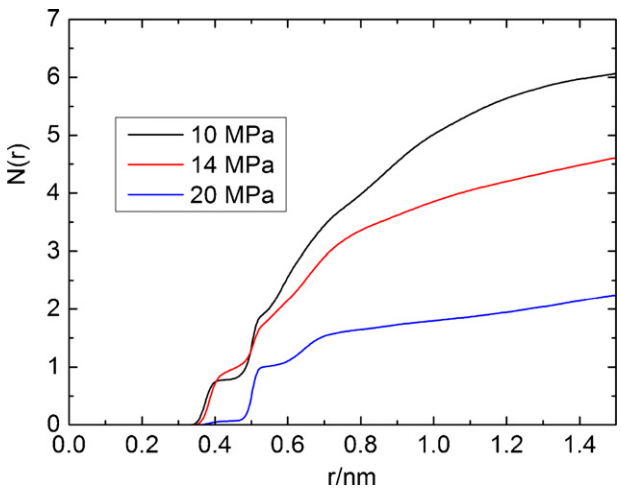

Fig. 8. Number integrals, N(r), for methanol molecules around o-HBA at pressure of 10 MPa (black line), 14 MPa (red line) and 20 MPa (blue line). (For interpretation of the references to color in this figure legend, the reader is referred to the web version of this article.)

3.3. Local mole fraction enhancement

The co-solvent cluster around the solute can form a more favorable local environment compared to the bulk solvent. Han and co-workers pointed out that the local environment around solute has an effect on the solubility enhancement [5]. Therefore the aggregation of methanol around m-HBA and o-HBA in supercritical CO_2 was examined at pressures 10, 14 and 20 MPa. Because the results obtained for both solutes are similar, we will only use the data from o-HBA for discussion. In Fig. 8, the number integrals for the methanol center of mass and o-HBA center of mass was calculated. It is found that the number integrals decrease from 10 to 20 MPa, suggesting that the increase in pressure reduces the aggregation of methanol molecules. The same conclusion was also obtained by Stubbs and Siepmann [26]. We also calculated the number integrals of CO_2 around o-HBA at pressures 10, 14 and 20 MPa (Fig. 9). It is found that the number integrals increase with the increase in pressure. In other words, with the increase in pressure more and more CO_2 molecules aggregate around o-HBA.

Using the number integrals as shown in Figs. 8 and 9, it is possible to determine a local mole fraction $x_{local,MeOH}(r)$ that is distance

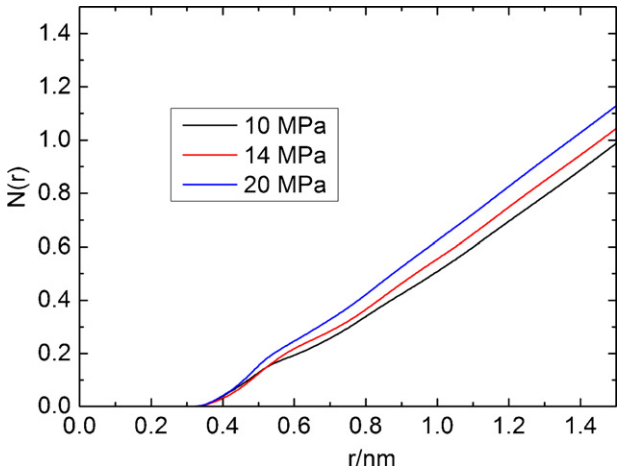

Fig. 9. Number integrals, N(r), for CO_2 around o-HBA at pressure of 10 MPa (black line), 14 MPa (red line) and 20 MPa (blue line). (For interpretation of the references to color in this figure legend, the reader is referred to the web version of this article.)

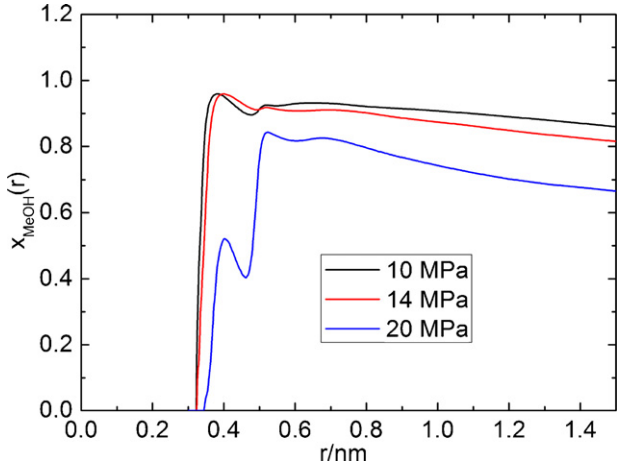

Fig. 10. Local mole fraction of methanol around o-HBA at T = 328 K, 10 MPa (black line), 14 MPa (red line) and 20 MPa (blue line). (For interpretation of the references to color in this figure legend, the reader is referred to the web version of this article.)

dependent and defined by the equation as described in literature [26].

$$x_{\text{local, MeOH}}(r) = \frac{N_{\text{neighbors, MeOH}}(r)}{N_{\text{neighbors, MeOH}}(r) + N_{\text{neighbors, CO}_2}(r)} \quad (3)$$

with $N_{\text{neighbors,A}}(r)$ being the average number of neighbors of type A inside a sphere of radius r around o-HBA. A plot of the local mole fractions at 328 K and different pressures is shown in Fig. 10. It is found that the local mole fraction is enhanced at r = 0.4 nm. When the pressure increases from 10 to 14 MPa, the decrease of the local mole fraction enhancement is very small. When the pressure reaches 20 MPa, the local mole fraction enhancement decreases significantly. It means that with the pressure increasing, the local mole fraction enhancement around o-HBA decreases. This was mainly due to the increase of the number of CO_2 around o-HBA and the decrease of the number of methanol around o-HBA with the pressure increasing, which can be seen from Figs. 8 and 9. The change of local mole fraction enhancement of methanol around o-HBA with pressure signals that the increase of pressure could diminish the aggregation of methanol around o-HBA.

4. Conclusions

The solvation structures of o-/m-HBA in CO_2 and methanol mixtures were investigated by molecular dynamics simulation. The SDFs and RDFs at 14 MPa show that methanol clusters were formed around the solutes through hydrogen bonding. The methanol molecules were preferred to aggregate around carboxyl group and hydroxyl group of m-HBA, but around only hydroxyl group of o-HBA.

Based on the analysis of the total number of hydrogen bondings, the interaction between m-HBA and methanol was much stronger than that between o-HBA and methanol, and with increasing CO_2 pressure it does not change for the former, but decreases for the latter. The calculation of the local mole fraction of methanol around solutes revealed that increasing pressure could diminish the aggregation of methanol around solutes. The decreased enhancement of solubility can be ascribed to the following two factors, i.e., the decease of hydrogen bonding and the less aggregation of methanol around solutes with the increase of pressure. In a word, the solute structure and interaction between co-solvent and solute were very important for solvation, which would have implications for extraction and purification techniques.

Acknowledgments

The authors gratefully acknowledge the financial support from the NSFC 20873139 and the One Hundred Talent Program of CAS.

Appendix A. Supplementary data

Supplementary data associated with this article can be found, in the online version, at doi:10.1016/j.supflu.2011.06.008.

References

[1] Y. Ikushima, M. Arai, K. Hatekeda, S. Ito, N. Saito, T.D. Goto, Selective extraction of a mixture of stearic, oleic, linoleic and linolenic acid methyl esters with supercritical carbon dioxide using a gas-flow method, Journal of Chemical Engineering of Japan 21 (1988) 439–441.
[2] E. Kiran, P.G. Debenedetti, C.J. Peters (Eds.), Supercritical Fluids: Fundamentals and Applications, NATO ASI Science Series E, Applied Sciences, vol. 366, Kluwer Academic Publishers, Dordrecht, The Netherlands, 2000.
[3] C.A. Eckert, B.L. Knutson, P.G. Debenedetti, Supercritical fluids as solvents for chemical and materials processing, Nature 383 (1996) 313–318.
[4] S.C. Tucker, Solvent density inhomogeneities in supercritical fluids, Chemical Reviews 99 (1999) 391–418.
[5] X. Zhang, B. Han, Z. Hou, J. Zhang, Z. Liu, T. Jiang, J. He, H. Li, Why do co-solvents enhance the solubility of solutes in supercritical fluids? New evidence and opinion, Chemistry: A European Journal 8 (2002) 5107–5111.
[6] J. Zagrobelny, F.V. Bright, Probing solute–entrainer interactions in matrix-modified supercritical CO_2, Journal of the American Chemical Society 115 (1993) 701–707.
[7] M. Yamamoto, Y. Iwai, T. Nakajima, Y. Arai, Fourier transform infrared study on hydrogen bonding species of carboxylic acids in supercritical carbon dioxide with ethanol, Journal of Physical Chemistry A 103 (1999) 3525–3529.
[8] D.L. Tomasko, B.L. Knutson, F. Pouillot, C.L. Liotta, C.A. Eckert, Spectroscopic study of structure and interactions in cosolvent-modified supercritical fluids, Journal of Physical Chemistry 97 (1993) 11823–11834.
[9] J. Ke, S. Jin, B. Han, H. Yan, D. Shen, Hydrogen bonding of some organic acid in supercritical CO_2 with polar cosolvents, Journal of Supercritical Fluids 11 (1997) 53–60.
[10] K.E. Anderson, J.I. Siepmann, Solubility in supercritical carbon dioxide: importance of the poynting correction and entrainer effects, Journal of Physical Chemistry B 112 (2008) 11374–11380.
[11] I. Skarmoutsos, D. Dellis, J. Samios, Investigation of the local composition enhancement and related dynamics in supercritical CO_2-cosolvent mixtures via computer simulation: the case of ethanol in CO_2, Journal of Chemical Physics 126 (2007) 224503.
[12] J.L. Gohres, C.L. Shukla, A.V. Popov, R. Hernandez, C.L. Liotta, C.A. Eckert, Effects of solute structure on local solvation and solvent interactions: results from UV/Vis spectroscopy and molecular dynamics simulations, Journal of Physical Chemistry B 112 (2008) 14993–14998.
[13] C.D. Saquing, F.P. Lucien, N.R. Foster, Steric effects and preferential interactions in supercritical carbon dioxide, Industrial and Engineering Chemistry Research 37 (1998) 4190–4197.
[14] H. Bekker, H.J.C. Berendsen, E.J. Dijkstra, S. Achterop, R. van Drunen, D. van der Spoel, A. Sijbers, H. Keegstra, B. Reitsma, M.K.R. Renardus, GROMACS: a parallel computer for molecular dynamics simulations, in: R.A. de Groot, J. Nadrchal (Eds.), Physics Computing 92 (Singapore, 1993), World Scientific, 1993.
[15] H.J.C. Berendsen, D. van der Spoel, R. van Drunen, GROMACS: a message-passing parallel molecular dynamics implementation, Computer Physics Communications 91 (1995) 43–56.
[16] E. Lindahl, B. Hess, D. van der Spoel, GROMACS 3.0: a package for molecular simulation and trajectory analysis, Journal of Molecular Modeling 7 (2001) 306–317.
[17] D. van der Spoel, E. Lindahl, B. Hess, G. Groenhof, A.E. Mark, H.J.C. Berendsen, GROMACS: fast, flexible and free, Journal of Comparative Chemistry 26 (2005) 1701–1718.
[18] B. Hess, C. Kutzner, D. van der Spoel, E. Lindahl, GROMACS 4: algorithms for highly efficient, load-balanced, and scalable molecular simulation, Journal of Chemistry Theory and Computation 4 (2008) 435–447.
[19] J. Harris, K. Yung, Carbon dioxide's liquid-vapor coexistence curve and critical properties as predicted by a simple molecular model, Journal of Physical Chemistry 99 (1995) 12021–12024.
[20] B. Chen, J.J. Potoff, J.I. Siepmann, Monte carlo calculations for alcohols and their mixtures with alkanes. Transferable potentials for phase equilibria. 5. United-atom description of primary, secondary, and tertiary alcohols, Journal of Physical Chemistry B 105 (2001) 3093–3104.
[21] W.D. Cornell, P. Cieplak, C.I. Bayly, I.R. Gould, K.M. Merz Jr., D.M. Ferguson, D.C. Spellmeyer, T. Fox, J.W. Caldwell, P.A. Kollman, A second generation force field for the simulation of proteins, nucleic acids, and organic molecules, Journal of American Chemical Society 117 (1995) 5179–5197.
[22] K.P. Johnston, S. Kim, J. Combes, Spectroscopic determination of solvent strength and structure in supercritical fluid mixtures: a review,

in: K.P. Johnston, J.M.L. Penninger (Eds.), Supercritical Fluid Science and Technology, American Chemical Society, Washington, DC, 1989, pp. 52–70.
[23] P.G. Kusalik, I.M. Svishchev, The spatial structure in liquid water, Science 265 (1994) 1219–1221.
[24] I.M. Svishchev, P.G. Kusalik, Crystallization of liquid water in a molecular dynamics simulation, Physical Review Letters 73 (1994) 975–978.
[25] A. Chandra, Dynamical behavior of anion–water and water–water hydrogen bonds in aqueous electrolyte solutions: a molecular dynamics study, Journal of Physical Chemistry B 107 (2003) 3899–3906.
[26] J.M. Stubbs, J.I. Siepmann, Binary phase behavior and aggregation of dilute methanol in supercritical carbon dioxide: a Monte Carlo simulation study, Journal of Chemical Physics 121 (2004) 1525–1534.